JACS
JOURNAL OF THE AMERICAN CHEMICAL SOCIETY
Article
pubs.acs.org/JACS

Carboxylate-Assisted C(sp^3)–H Activation in Olefin Metathesis-Relevant Ruthenium Complexes

Jeffrey S. Cannon,[†] Lufeng Zou,[‡] Peng Liu,[‡] Yu Lan,[‡] Daniel J. O'Leary,*[,§] K. N. Houk,*[,‡] and Robert H. Grubbs*[,†]

[†]Arnold and Mabel Beckman Laboratory of Chemical Synthesis, Division of Chemistry and Chemical Engineering, California Institute of Technology, Pasadena, California 91125, United States

[‡]Department of Chemistry and Biochemistry, University of California, Los Angeles, California 90095-1569, United States

[§]Department of Chemistry, Pomona College, Claremont, California 91711, United States

Supporting Information

ABSTRACT: The mechanism of C–H activation at metathesis-relevant ruthenium(II) benzylidene complexes was studied both experimentally and computationally. Synthesis of a ruthenium dicarboxylate at a low temperature allowed for direct observation of the C–H activation step, independent of the initial anionic ligand-exchange reactions. A first-order reaction supports an intramolecular concerted metalation–deprotonation mechanism with $\Delta G^{\ddagger}_{298K}$ = 22.2 ± 0.1 kcal·mol^{-1} for the parent *N*-adamantyl-*N*′-mesityl complex. An experimentally determined $\Delta S^{\ddagger}$ = −5.2 ± 2.6 eu supports a highly ordered transition state for carboxylate-assisted C(sp^3)–H activation. Experimental results, including measurement of a large primary kinetic isotope effect (k_H/k_D = 8.1 ± 1.7), agree closely with a computed six-membered carboxylate-assisted C–H activation mechanism where the deprotonating carboxylate adopts a pseudo-apical geometry, displacing the aryl ether chelate. The rate of cyclometalation was found to be influenced by both the electronics of the assisting carboxylate and the ruthenium ligand environment.

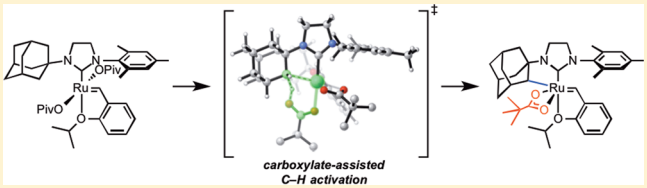

INTRODUCTION

The activation of C–H bonds by transition metal complexes has become an important, growing field in organic synthesis.[1] At the core of this field is the need to understand the general mechanisms of the C–H activation step in order to harness the reactivity for synthetic processes. As a result, mechanistic and computational studies have been of great interest to organic and inorganic chemists in order to elucidate the mechanisms of C–H activation reactions by transition metals, including Pd,[1b,2] Ir,[3] Rh,[4] Ru,[5] and others.[6]

Carboxylate-assisted C–H activation has recently garnered attention as a generally mild method for C–H activation at transition metal centers.[1a,c] The use of carboxylates in catalytic C–H activation reactions has grown tremendously in recent years, and several reports investigating the mechanism have appeared.[7] The majority of these reactions involve activation of aromatic or vinylic C(sp^2)–H bonds, and only sparing examples of carboxylate-assisted C(sp^3)–H activation have been reported.[1c] Computational and mechanistic studies have been primarily focused on palladium carboxylate-catalyzed C–H activations, which often involve a concerted metalation–deprotonation (CMD) mechanism with a six-membered transition state.[2e,i,7d,8] Activation of C(sp^3)–H bonds with ruthenium complexes is particularly rare[9] and typically occurs through C–H oxidative addition to ruthenium[9n,10] or C–H radical abstraction with a ruthenium-oxo/nitrenoid.[11] The mechanism of carboxylate-mediated C(sp^2)–H activation at ruthenium has been studied in only a single family of complexes.[5d,12] The CMD C–H activation mechanism, which is particularly common with palladium carboxylate catalysts, is largely unexplored with ruthenium. Furthermore, inner-sphere activation of methylene C(sp^3)–H bonds is quite rare and is essentially unprecedented for ruthenium.

We recently reported the synthesis of a new family of cyclometalated ruthenium benzylidene complexes (**1**–**3**, Figure 1).[13] These ruthenium complexes were found to be highly selective for *Z*-olefins (typically >90% *Z*) in a number of olefin metathesis reactions, including macrocyclic ring-closing metathesis,[14] cross metathesis,[15] asymmetric ring-opening cross metathesis,[16] ring-opening metathesis polymerization,[13d] and ethenolysis reactions.[17] These findings were complementary to the reactivity of molybdenum and tungsten catalysts reported by Schrock and Hoveyda.[18]

Cyclometalated complexes **1**–**3** are highly interesting organometallic species. These complexes contain a stable Ru–C bond in the presence of a reactive ruthenium alkylidene. Previous observations of C–H bond activation in ruthenium alkylidene complexes led to decomposition of the Ru–C bond, typically through insertion into the alkylidene followed by hydride elimination reactions.[19] The stable cyclometalated

Received: March 3, 2014
Published: April 14, 2014

   dx.doi.org/10.1021/ja5021958 | *J. Am. Chem. Soc.* 2014, 136, 6733–6743

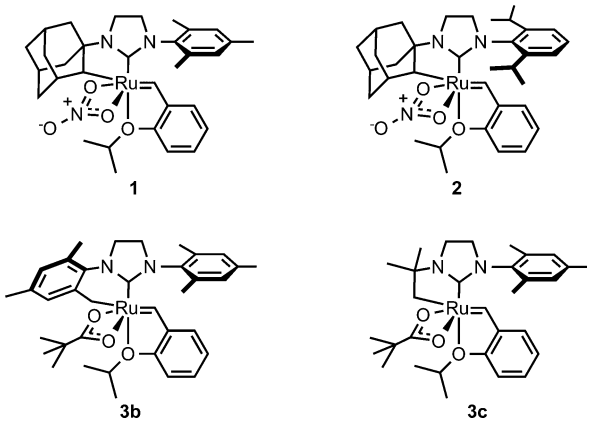

Figure 1. Cyclometalated ruthenium metathesis catalysts.

Scheme 1. Synthesis of Cyclometalated Complexes

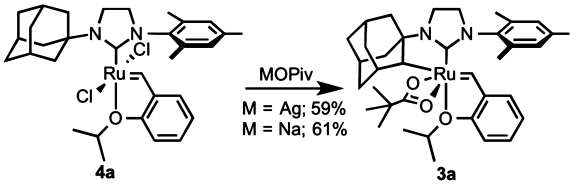

complexes are synthesized by the reaction of a ruthenium dichloride complex with an excess of a pivalate salt (Scheme 1). While silver pivalate was found to efficiently provide cyclometalated complexes,[13a,b] product stability to the reaction conditions was improved by the use of sodium carboxylate salts.[13c] In light of this initial advance in cyclometalation methodology, kinetic studies on the cyclometalation of these complexes would enable the synthesis of a broader family of potentially useful ruthenium alkylidene complexes. Furthermore, because of the high stability of complexes **1**–**3** and the lack of in-depth kinetic studies on the activation of C(sp^3)–H bonds, it was envisioned that an investigation into the reactivity of complexes **4** toward cyclometalation would be a valuable addition to the C–H activation literature.

This report contains a detailed study of the mechanism of C(sp^3)–H activation at ruthenium(II) alkylidenes. By complementing direct observation of the elementary C–H activation step with density functional theory (DFT) studies, unique and important features of a carboxylate-assisted CMD at metathesis-relevant ruthenium(II) complexes could be elucidated.

RESULTS

Dichloride Reactivity. Initial experiments were conducted to investigate the kinetics of C–H activation as it proceeds from the dichloride complex (**4**, Scheme 2). Complexes **4** were exposed to 10 equiv of sodium pivalate as a solution in 1:1 THF-d_8:CD_3OD at 40 °C. Both THF and methanol are required for this reaction because of the limited solubility of complexes **4** and **3** in pure methanol and of sodium pivalate in pure THF. The reaction progress could be easily monitored by observation of benzylidene peaks (δ 15–20 ppm) in ^{1}H NMR spectra.

These reactions were characterized by a first-order decay of the starting complex, with a buildup of two intermediates identified as the mono- and dicarboxylates resulting from salt exchange with the chloride ligands (Figure 2). This initial

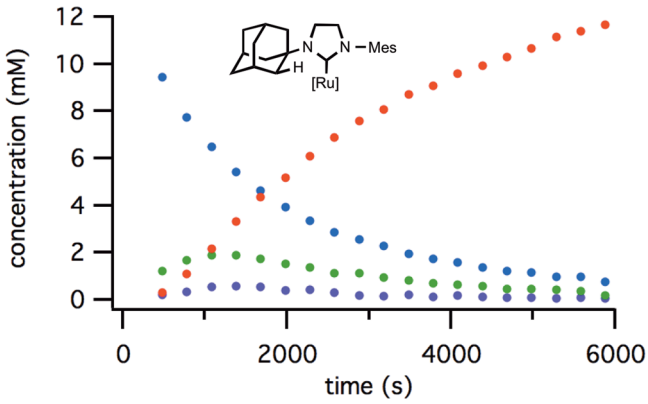

Figure 2. Reaction progress of cyclometalation of complex **4a**: blue = [**4a**], green = [**5a**], purple = [**6a**], red = [**3a**].

ligand exchange resulted in a short induction period prior to the generation of cyclometalated complex **3**. In the specific case of *N*-adamantyl complex **4a**, the salt metathesis was slow, generating low concentrations of mono- and dicarboxylate species.

The C–H activation of mesityl complex **4b** was also followed by ^{1}H NMR spectroscopy (Figure 3). The production of **3b**

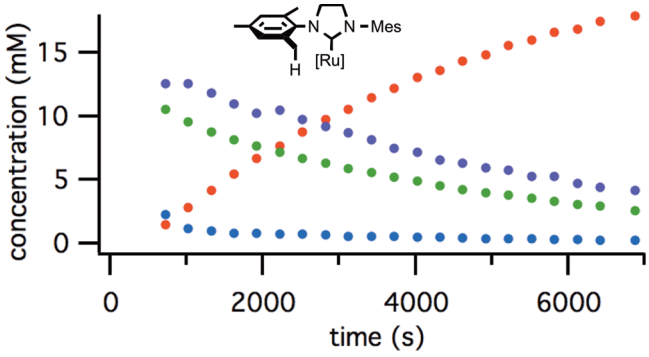

Figure 3. Reaction progress of cyclometalation of complex **4b**: blue = [**4b**], green = [**5b**], purple = [**6b**], red = [**3b**].

Scheme 2. Proposed Mechanism of C–H Activation of Ruthenium Complex 4a

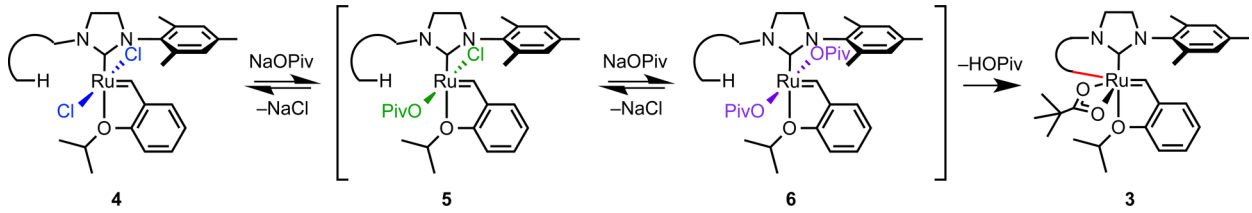

dx.doi.org/10.1021/ja5021958 | J. Am. Chem. Soc. 2014, 136, 6733–6743

was characterized by the same induction period as observed with complex **3a**; however, the equilibrium more heavily favored the carboxylate complexes. In this case, equilibrium was also reached more rapidly, with only 3% of the dichloride complex observable at the first time point.

Cyclometalation of *N*-*t*-Bu-*N*′-mesityl-substituted NHC ruthenium complex **4c** was also monitored by ^{1}H NMR spectroscopy (Figure 4). Much like complex **4a**, ligand

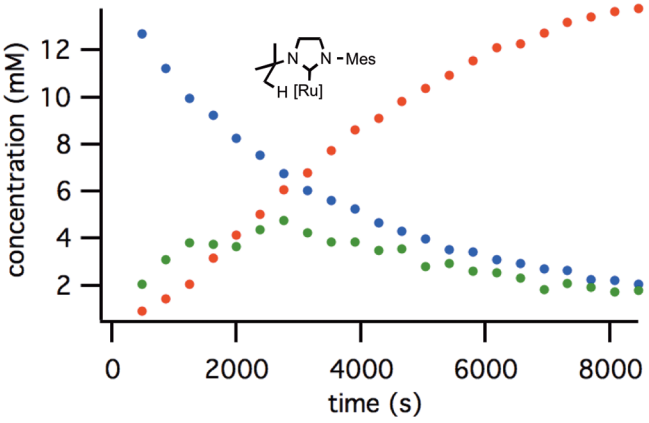

Figure 4. Reaction progress of cyclometalation of complex **4c**: blue = [**4c**], green = [**5c**], red = [**3c**]; **6c** was not observed.

exchange to provide the dipivalate was slow, and only the monocarboxylate complex could be observed in the reaction mixture. The overall rate was only slightly faster than for the previous complexes.

The C−H activation of a complex with *N*-adamantyl-*N*′-2,6-diisopropylphenyl (DIPP, **4d**) substitution of the NHC ligand was also monitored. It was found to possess a notably decreased rate when compared to complexes **4a**−**c**. For instance, whereas cyclometalation of complex **4a** reaches completion after approximately 4 h, DIPP-substituted complex **4d** is not fully consumed until after 96 h. During the course of this experiment, negligible amounts of carboxylate-ligated complexes **5d** or **6d** were observed.

In order to study the nature of the salt-exchange steps that precede C−H activation, monochloride monopivalate complex **5b** was synthesized (Scheme 3).[13e] Complex **5b** is a stable green solid that does not undergo ligand disproportionation in THF/MeOH solution. Furthermore, no cyclometalation was

Scheme 3. Synthesis and Reactivity of Monopivalate Complex 5b

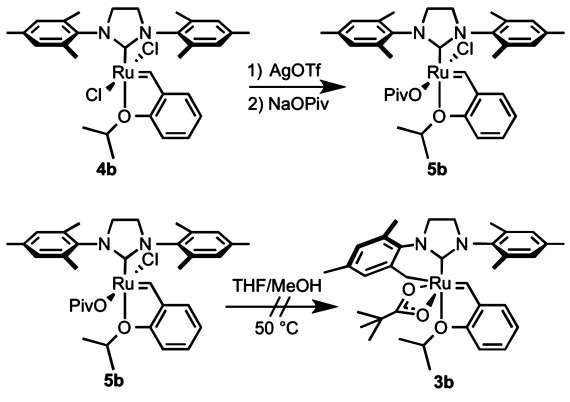

observed upon exposure of complex **5b** to the reaction conditions in the absence of excess sodium pivalate. Addition of sodium pivalate (9 equiv) to a THF/MeOH solution of **5b** provides cyclometalated product **3b** after heating to 40 °C, indicating the intermediacy of monocarboxylate **5b** in the formation of **3b**. It should also be noted that C(sp^2)−H activation occurs competitively at complexes **4** with aryl groups bearing ortho hydrogen atoms; however, these complexes rapidly decompose upon insertion into the benzylidene.[19a]

Activation of Dicarboxylate Complexes. In order to study the central C−H activation step, a method for the independent synthesis of dipivalates **6** was developed. It was envisioned that replacing the chloride ligands with more rapidly exchanged X-type ligands would allow dicarboxylates to be synthesized at temperatures where C−H activation was sufficiently retarded (Scheme 4). To achieve this, dichlorides

Scheme 4. Synthesis and C−H Activation of Dicarboxylate Precursor for Kinetic Studies

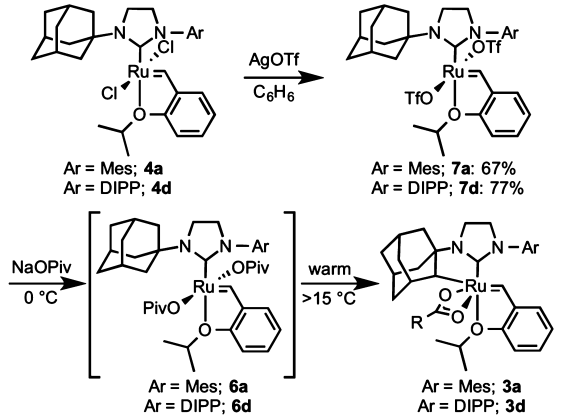

4 were treated with 4 equiv of silver triflate in benzene. Stable bis-triflate complexes **7** were isolated after removal of silver salts by filtration of the reaction mixture. Both *N*-mesityl complex **7a** and *N*-DIPP complex **7d** could be synthesized in this manner. Though the bis-triflate analogue of mesityl complex **4b** is known, it was found to be unstable to cyclometalation conditions.[13e,20] The bis-triflate analogue of *tert*-butyl complex **4c** could not be synthesized. Immediate general decomposition of **4c** was observed upon exposure to silver triflate. Importantly, triflates **7** did not undergo C−H activation upon heating.

It was found that bis-triflate **7a** could be treated with as little as 3 equiv of sodium carboxylate salts to cleanly generate dicarboxylate **6a** in situ. Complete conversion to the dicarboxylate was typically achieved in under 30 min at 0 °C, and no cyclometalated products (e.g., **3a**) were generated within this time frame. While a THF/MeOH solvent mixture was not necessary to observe C(sp^3)−H activation (reaction could be achieved in benzene or pure THF), 1:1 THF/MeOH was chosen for these studies to enable both increased reaction homogeneity and ready comparison to reactions that proceed from dichlorides **4**.

The C−H activation of dicarboxylate **6a** was then directly observed after the solution was warmed to the reaction temperature. The reaction was found to be first order in dicarboxylate, with rate constant $k_{313K} = (1.6 \pm 0.1) \times 10^{-3}$ s^{-1}. A similar procedure was used to study the C−H activation of *N*-DIPP complex **6d**, and the rate constant was determined to be $k_{313K} = (1.4 \pm 0.2) \times 10^{-3}$ s^{-1}.

dx.doi.org/10.1021/ja5021958 | J. Am. Chem. Soc. 2014, 136, 6733−6743

Eyring Analysis. The method described in Scheme 4 was used to conduct an Eyring analysis of the C−H activation step (Figure 5). The reaction was monitored over a temperature range from 15 to 55 °C. A linear Eyring plot was generated with an excellent fit. Analysis of the slope of the plot and the *y*-intercept provided the energies of activation. It was found that the conversion of dipivalate **6a** to cyclometalated ruthenium benzylidene **3a** requires $\Delta H^{\ddagger}$ = 20.6 ± 0.8 kcal·mol^{-1}, with a negative entropy of activation, $\Delta S^{\ddagger}$ = −5.2 ± 2.6 eu. This provides a Gibbs free energy of activation, $\Delta G^{\ddagger}$ = 22.2 ± 0.1 kcal·mol^{-1} at 25 °C.

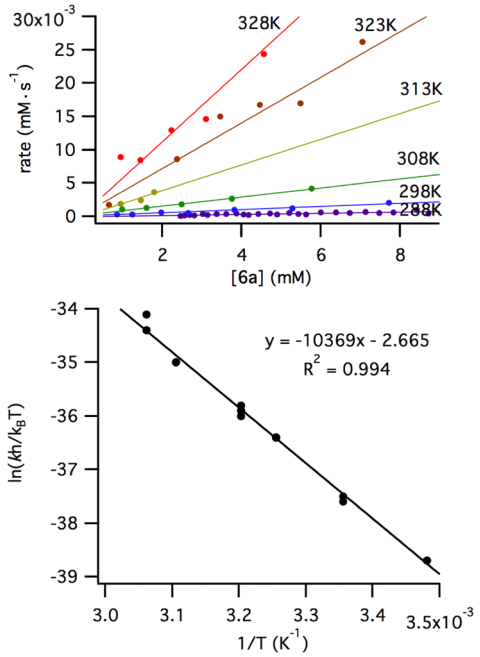

Figure 5. Rate plots (top) and Eyring analysis (bottom) of cyclometalation of ruthenium complex **6a**.

Linear Free Energy Relationships. The effect of the electronic properties of the carboxylate was probed by establishing a linear free energy relationship between the Hammett substituent constants and the rate of cyclometalation. Previous computational Hammett studies revealed that C−H *σ*-bond metathesis with Tp(CO)Ru(II)−X (X = R, NH_2, OR, or BOR_2) is insensitive to the electronic property of the C−H bond.[21] Dicarboxylates **8a−e** were synthesized by using the sodium salts of various 4-substituted benzoic acids (Figure 6). While the rate of activation by substituted benzoic acids correlated only moderately with Hammett σ values, the correlation was increased when σ^{+} values were utilized. A moderately negative ρ value of −0.24 was observed (Figure 6).

The electronic influence of substitution of the benzylidene chelate on the rate of C−H activation was also investigated (Figure 7). Substitution of the benzylidene chelate has demonstrated effects on the initiation rates of metathesis catalysts.[22] Using the Hammett σ_{para} values, substitution of the 4-position of the benzylidene chelate provided insignificant correlation. The strongest correlation was observed when using the corresponding σ_{meta} values. This observation indicates a much stronger influence of benzylidene substituents on the 2-position of the chelate, inductively to the ruthenium center. The ρ value for this plot was found to be +0.53.

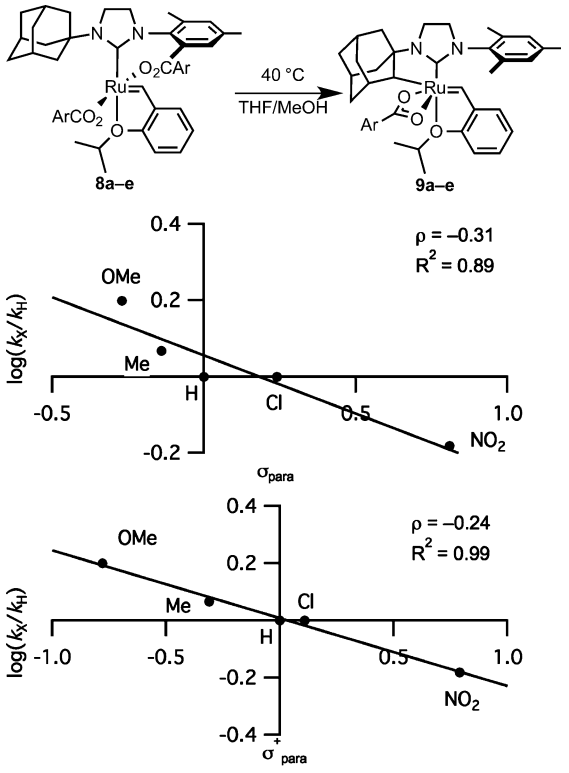

Figure 6. Linear free energy relationships with ruthenium dibenzoates **8a−e**.

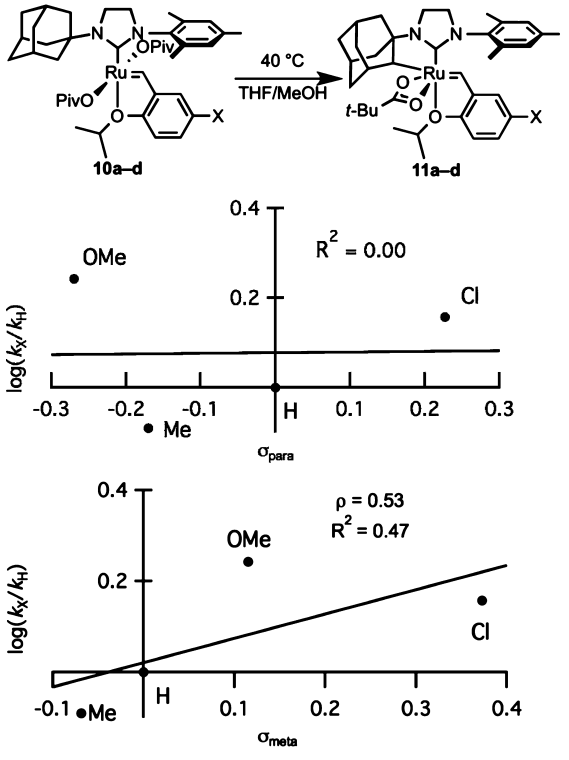

Figure 7. Linear free energy relationships with substituted ruthenium chelates **10a−d**.

Initiation rates of related dichloride complexes (**10a−d**; OPiv = Cl) were measured by observing the rate of decay of the benzylidene peak after the complex was treated with butyl vinyl ether.[23] While the initiation rates were also affected by the

dx.doi.org/10.1021/ja5021958 | J. Am. Chem. Soc. 2014, 136, 6733−6743

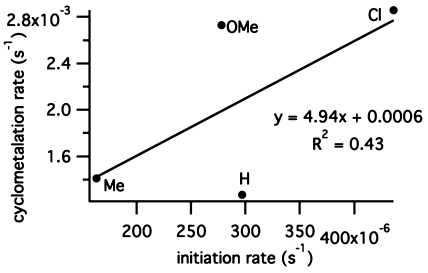

Figure 8. Relationship between initiation rate of dichlorides and rate of cyclometalation of dicarboxylates **3**.

Table 1. Kinetic Isotope Effects

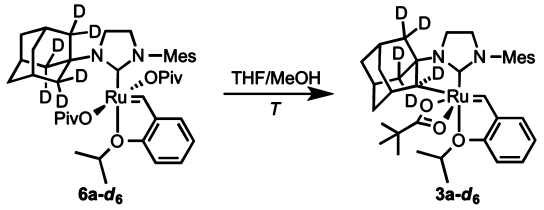

entry	k	T (°C)	value (s^{-1})[a]	KIE[a]
1	k_H	25	$(2.8 \pm 0.4) \times 10^{-4}$	8.1 ± 1.7
2	k_D	25	$(3.5 \pm 0.6) \times 10^{-5}$	
3	k_H	50	$(4.3 \pm 0.3) \times 10^{-3}$	6.4 ± 1.1
4	k_D	50	$(6.7 \pm 1) \times 10^{-4}$	

[a]Uncertainty reported with 90% confidence intervals.

electronic nature of the benzylidene chelate, the rate of C−H activation also has little correlation with the initiation rates of the related dichloride complexes (Figure 8). Initiation rates also did not correspond well with Hammett σ values.

Kinetic Isotope Effects. Kinetic isotope effects (KIEs) are a common measurement when studying the mechanism of C−H activation with transition metals.[24] In order to measure the KIE ($= k_H/k_D$) of C(sp^3)−H activation at these ruthenium complexes, deuterated dicarboxylate **6a**-d_6 was synthesized utilizing d_6-1-adamantylamine (Table 1). In separate experiments, the rates of C−H and C−D activation were measured. At 25 °C, KIE = 8.1 ± 1.7 was found. At an elevated temperature of 50 °C, the value was reduced to KIE = 6.4 ± 1.1.

Computational Studies on the Mechanism of C−H Activation. We performed DFT calculations to investigate the mechanism of the C−H activation pathways and to explain the effects of *N*-substituents on the reactivity and selectivity of C−H activation. The calculations were performed using the theoretical method that was found satisfactory in our recent computations with ruthenium metathesis catalysts.[17,19a,25] The geometries were optimized with B3LYP and the SDD basis set for Ru and 6-31G(d) for other atoms. Single-point energies were calculated with M06 and the SDD basis set for Ru and the 6-311+G(d,p) basis set for other atoms. The SMD solvation model was employed in the single-point energy calculations. THF was used as the solvent in the calculations. All calculations were performed with Gaussian 09.[26]

The calculations indicated that the C−H activation of ruthenium dichloride complex **4a** occurs through the pathway shown in blue in Figure 9. The monopivalate pathway shown in red is unfavorable (vide infra). The anion-exchange steps to replace both chlorides in **4a** with pivalates are exergonic by 1.4 and 4.0 kcal·mol^{-1}, respectively. The reaction with silver pivalate is expected to be even more favorable, driven by the formation of solid silver chloride precipitate. The pivalate in complex **5a** and both pivalates in complex **6a** are monoligated (Figure 10). The binding site *trans* to the benzylidene in these 16-electron complexes is blocked by the bulky *N*-adamantyl group.[27] The most favorable C−H activation pathway from the dipivalate complex **6a** involves rotation of the *o*-isopropoxyphenyl group (**12a-TS**) and dissociation of the Ru−O chelate to form **13a**, followed by deprotonation of the adamantyl C−H bond by a bottom-bound pivalate (**14a-TS-A**) via a CMD mechanism. The C−H activation step leads to a pivalic acid-bound complex **15a**, which then liberates pivalic acid and generates Ru−C cyclometalated catalyst **3a**. The rate-determining step was found to be the C−H activation via

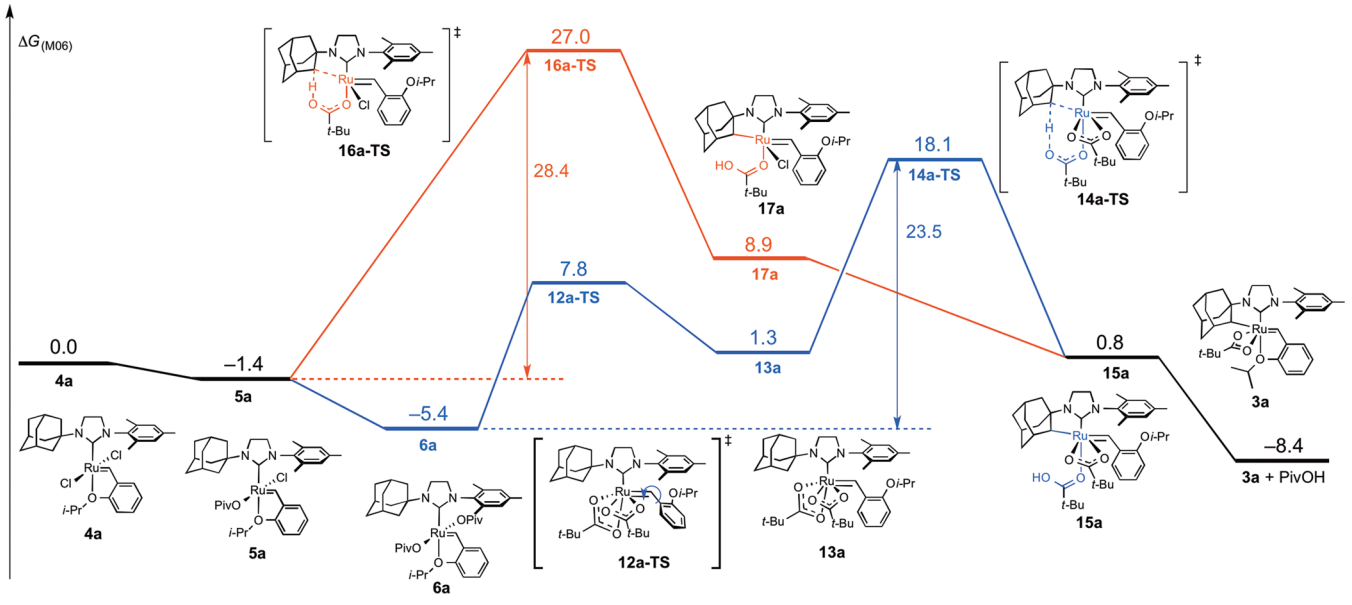

Figure 9. Free energy profile of the C−H activation of **4a** to form cyclometalated complex **3a**; all energies in kcal·mol^{-1} at 25 °C.

dx.doi.org/10.1021/ja5021958 | J. Am. Chem. Soc. 2014, 136, 6733−6743

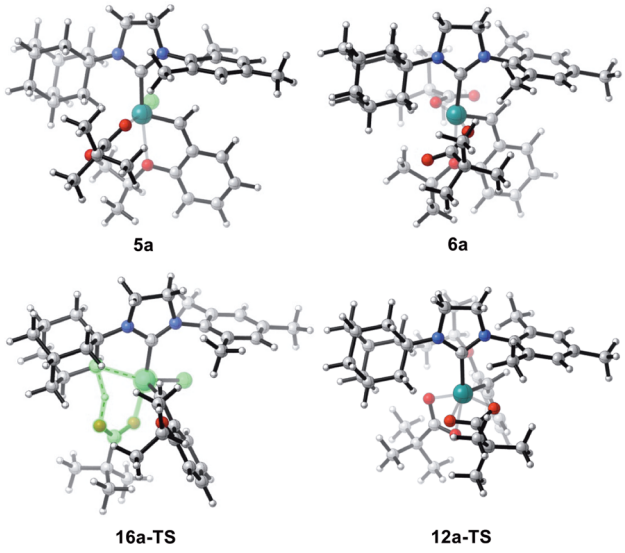

Figure 10. Optimized geometries of the monopivalate complex **5a**, dipivalate complex **6a**, the monopivalate C−H activation transition state **16a-TS**, and the *o*-isopropoxyphenyl rotation transition state **12a-TS**.

intramolecular CMD (**14a-TS-A**) and requires an overall free energy barrier of 23.5 kcal·mol^{-1} (**6a** → **14a-TS-A**).[28]

Several isomeric C−H activation transition states from the dipivalate complex **6a** have been calculated and are all found to be less stable than **14a-TS-A** (Figure 11). In **14a-TS-B**, the C−H bond is deprotonated by the pivalate bound to the side position (i.e., *cis* to the NHC). Although this orientation maintains the Ru−O(isopropoxy) chelation, such side-bound C−H activation is 6.9 kcal·mol^{-1} less favorable than the bottom-bound C−H activation. The four-membered-ring CMD transition state **14a-TS-C**, which is also referred to as *σ*-bond metathesis in the literature,[8c] is 14 kcal·mol^{-1} less favorable, as the oxygen coordinated to the Ru is less basic.[8a,29] An outer-sphere deprotonation transition state involving an unbound pivalate was also located (**14a-TS-D**) and is also unfavorable.[30] This is consistent with the preference for the six-membered CMD transition states in palladium acetate-catalyzed C−H activations.[2e,i,7d,8]

C−H(D) insertion KIEs were calculated[31] using the Bigeleisen−Mayer equation[32] with scaled (0.97)[33] harmonic frequencies obtained from B3LYP/LANL2DZ-6-31G* ground-state structure **6a** and transition structures **14a-TS-A−D** (Figure 12). B3LYP/SDD-6-31G(d) and M06/SDD-6-31G(d) models provided comparable KIE estimates for the **14a-TS-A** C−H insertion process at 25 °C (6.47 and 6.42, respectively). The computed KIEs decreased with increasing temperature (Figure 12) and were found to originate primarily from zero-point energy contributions.

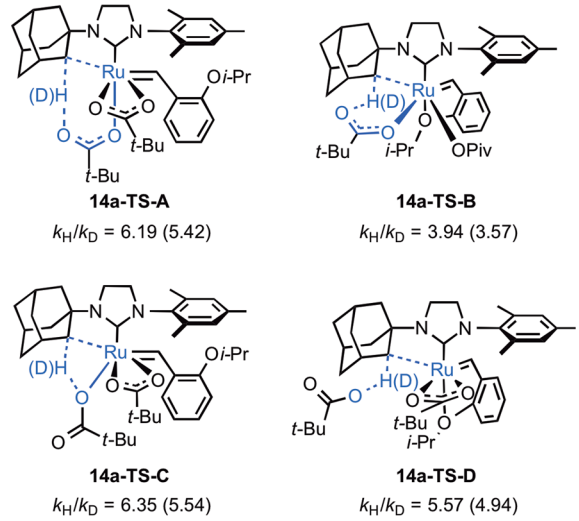

Figure 12. Kinetic isotope effects computed at 25 and 50 °C (in parentheses) for potential C−H(D) activation transition states.[31]

DISCUSSION

Salt Metathesis Affects the Overall Rate of Cyclometalation. The results outlined above support a general mechanism that requires two salt metathesis steps to preform a ruthenium dicarboxylate species. These salt metathesis events

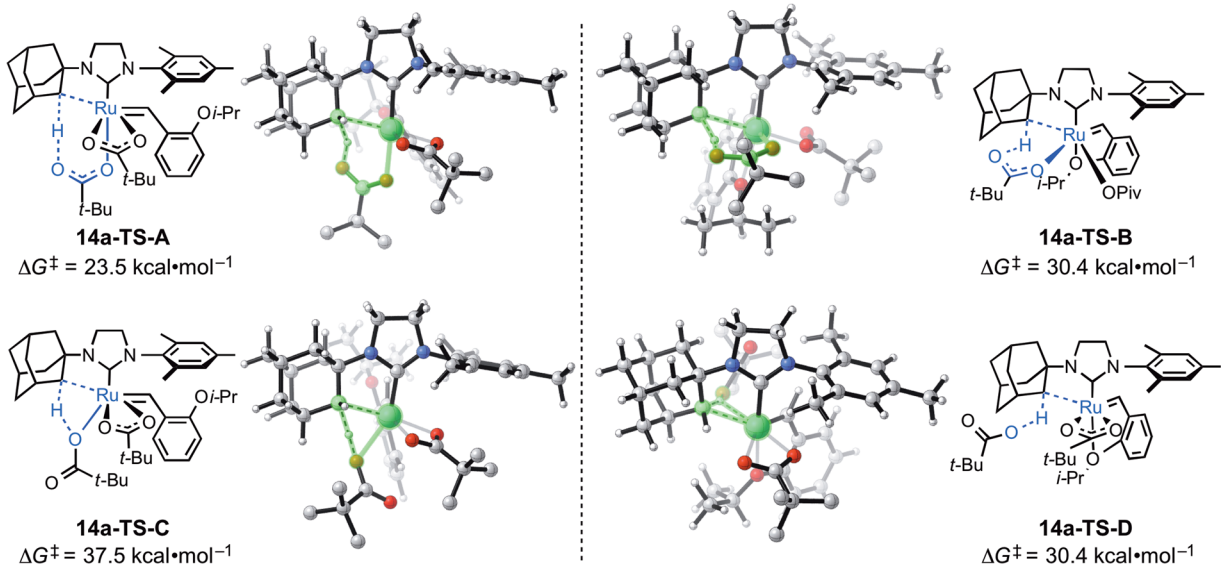

Figure 11. Four possible transition states for cyclometalation of dipivalate complex **6a**.

dx.doi.org/10.1021/ja5021958 | J. Am. Chem. Soc. 2014, 136, 6733−6743

have a profound effect on the observed rate of the cyclometalation reaction when starting from dichloride complexes (Table 2). For instance, the *N*-mesityl (**4a**) and

Table 2. Summary of Rate Information for Ruthenium Complexes 4 and 6[a]

entry	4	k from 4 ($\times 10^{-4}$ s^{-1})[b]	4:5:6[c]	k from 6 ($\times 10^{-3}$ s^{-1})[b]	calcd[d] k from 6 ($\times 10^{-4}$ s^{-1})
1	**4a**	2.7 ± 0.1	69:25:6	1.6 ± 0.1	2.7
2	**4b**	1.2 ± 0.1	3:38:59	–	0.084
3	**4c**	2.0 ± 0.1	56:43:<1	–	1.7×10^6
4	**4d**	<0.1	>98:<1:<1	1.4 ± 0.2	2.6

[a]All data from experiments conducted at 40 °C. [b]Uncertainty reported with 90% confidence intervals. [c]Relative concentrations of complexes at equilibrium. [d]See Supporting Information for details.

N-DIPP (**4d**) dichloride complexes differ greatly in observed rates of cyclometalation, but the rates for cyclometalation from the dipivalate complexes **6a** and **6d** are roughly equal (entries 1 and 4). This reduction in the cyclometalation rate of **4d** can be attributed to the poor equilibrium concentrations of reactive **6d** under the standard conditions. This same effect was also observed for complex **4c**, which is computationally expected to undergo cyclometalation at a much faster rate than **4a**. Interestingly, complex **4b** underwent cycloaddition at a rate similar to that of **4a**, although computations predicted the reaction from **6b** to be slower than that from **6a**.

In general, acceleration of the salt metathesis steps enhanced the overall rate of cyclometalation. For instance, cyclometalation occurred rapidly in the presence of silver pivalate salts as a result of the rapid nature of silver-mediated salt metathesis.[13b] This hypothesis is further supported by the observation that cyclometalation by exposure of triflate complexes **7** occurs rapidly at low temperature because of the more facile exchange of triflate ligands.

Dicarboxylate Stabilizes the Cyclometalation Transition State. Based on control experiments, only the ruthenium dicarboxylate species **6** is able to undergo C−H activation. This was further supported by computational evidence that the C−H activation transition state of monochloride-monocarboxylate **5a** is 8.9 kcal·mol^{-1} less stable than the corresponding transition state (**16a-TS**, red, vs **14a-TS**, blue, Figure 9). The monopivalate C−H activation also involves a bottom-bound six-membered transition state (**16a-TS**, Figure 10), similar to **14a-TS-A**. The lower energy of the dipivalate TS is in part due to the stronger binding energy of pivalate compared to chloride, as shown in the ground-state structures (**6a** vs **5a**). Additionally, the pivalate is bound to ruthenium in a κ^2 fashion in **14a-TS-A** and the final product **3a**. This binding mode offers additional stabilization compared to the κ^1 pivalate species prior to the C−H activation (**5a** and **6a**). In the reaction with monopivalate, there is no such stabilization in the cyclometalation transition state **16a-TS**, since the bidentate-bound pivalate is now replaced with chloride.

In addition, the chelating carboxylate ligand allows for further stabilization of the de-chelation of the benzylidene chelate (i.e., **13a**). Since the most energetically favorable cyclometalation transition state involves a pseudo-apically oriented carboxylate, the additional carboxylate ligand avoids any unstable 14-electron complexes involved in achieving the required transition-state geometry.

Rate of Cyclometalation Can Be Tuned Electronically. Experimental data reveal some of the electronic characteristics of the C−H activation reaction. The carboxylate ligand acts as a base, as indicated by the negative ρ value for the linear free energy relationship of ruthenium dibenzoates in the C−H activation reaction (Figure 6). Additionally, the stronger correlation to the σ^+ value suggests an accumulation of positive charge at the carboxylate carbon that is stabilized by resonance with the aromatic system. These results are supported by computational evidence that more basic carboxylates have lower activation barriers to C−H activation (Table 3).[34]

Table 3. Activation Free Energies (at 25 °C) for Cyclometalation with Different Carboxylate Ligands

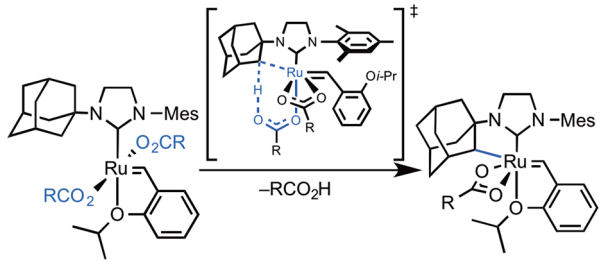

entry	R	dicarboxylate	$\Delta G^{\ddagger}$ (kcal·mol^{-1})	pK_a
1	*t*-Bu	**6a**	23.5	5.03
2	Me	**18a**	24.0	4.76
3	Ph	**8a**	26.2	4.20

Natural population analysis (NPA) calculations of **14a-TS-A** indicated polarization of the C−H bond being cleaved: the negative charge at C increases by −0.09, while the positive charge at H increases by +0.23 relative to that of dicarboxylate **6a**.[35] These electronic characteristics further support the CMD mechanism with the carboxylate acting as a base.

The electronic effects of the benzylidene chelate also reveal some characteristics of the ruthenium center during the C−H activation step. The lack of a strong correlation to either the σ_{para} or σ_{meta} values for substituents at the 4-position of the benzylidene chelate indicates a subtle competing effect of the electronics at both the chelating oxygen (σ_{para} values) and the ruthenium benzylidene (σ_{meta} values). Though a stronger correlation to the σ_{meta} values with a positive ρ value supports an increased importance of electron deficiency at ruthenium over the lability of the chelate, definitive conclusions cannot be drawn from the current experimental data. In addition, computations indicate no correlation between the benzylidene de-chelation energy and the C−H activation rate with different benzylidene chelates, **10a−d**.[36] These conclusions are further muddied by the absence of a correlation between the initiation rates of dichlorides and the rates of cyclometalation of the corresponding dipivalate complexes **10a−d**, even though both reactions include de-chelation of the isopropyl ether as a key organizational step.

The importance of increased positive charge at the ruthenium center on the observed rate of the reaction (Figure 7) agrees with the requirement of a dicarboxylate species. The additional electronic stabilization provided by the κ^2 pivalate ligand would stabilize the electrophilic character of the ruthenium center. This is further supported by the reduction in positive charge at ruthenium by −0.16 in the transition state, as calculated by natural population analysis. This reduction in positive charge indicates an accumulation of electrons

dx.doi.org/10.1021/ja5021958 | J. Am. Chem. Soc. 2014, 136, 6733−6743

throughout the reaction, a feature that would be more favorable for a more electron-deficient ruthenium center.

Pseudo-Apically Oriented Six-Membered Concerted Metalation–Deprotonation Transition-State Geometry. The results reported above support the reorganization of ligands to a transition-state geometry as depicted in **14a-TS-A** (Figure 11). The close agreement between the experimental $\Delta G^{\ddagger}_{298K}$ = 22.2 ± 0.1 kcal·mol^{-1} and the computed $\Delta G^{\ddagger}$ = 23.5 kcal·mol^{-1} lends credence to the computed geometries. Computations indicated that other isomeric C–H activation transition states (**14a-TS-B/C/D**) are at least 6.9 kcal·mol^{-1} less favorable than **14a-TS-A**. Furthermore, the large, negative $\Delta S^{\ddagger}$ = −5.2 ± 2.6 eu obtained from the Eyring analysis supports a highly ordered cyclic transition state.

The pseudo-apical orientation of the deprotonating carboxylate in **14a-TS-A** is also supported by the KIE (Figure 12). The measured KIE = 8.1 ± 1.7 more closely reflects the computed isotope effects for the two transition states that involve ligand reorganization to place the participating carboxylate in a pseudo-apical position (**14a-TS-A** and **14a-TS-C**). Furthermore, the small and computationally predicted reduction to KIE = 6.4 ± 1.1 at elevated temperatures excludes significant tunneling and lends additional support for this mechanism of C–H insertion.

Site Selectivity of C–H Activation Is Controlled by Steric Effects. In the C–H activation reaction with unsymmetrically substituted NHC complexes such as *N*-adamantyl-*N*′-mesityl complex **6a**, it is somewhat unexpected that the weaker mesityl C–H bond remains intact while reaction occurs exclusively at the adamantyl C–H bond.[2e,f,37] In addition, the C–H activation in the stereogenic-at-Ru complex is completely stereoselective. Only a single diastereomer of **3a** is observed, in which the benzylidene is *anti* to the C–H bond on the adamantyl (Scheme 5). Computations predicted the same major C–H activation product (**3a**) as that observed in experiment. Activation of the mesityl C–H bond requires 27.7 kcal·mol^{-1} (**14-TS-F**), 4.2 kcal·mol^{-1} higher than the adamantyl C–H bond activation (**14a-TS-A**). The transition state in which the benzylidene is *syn* to the C–H bond on the adamantyl (**14a-TS-E**) is 2.1 kcal·mol^{-1} less stable. The major product **3a** is also thermodynamically the most stable among the three isomers.

Steric interactions in the transition state disfavor activation of the weaker benzylic C–H bonds of **6a** (Figure 13). There is substantial distortion in **14a-TS-F** because of the steric repulsion between one of the ortho Me groups on the mesityl and a methylene group on the NHC backbone. This repulsion prevents the other methyl substituent from rotating into proximity of the ruthenium center. In addition, orientation of the bulky *N*-adamantyl group toward the benzylidene leads to steric interactions with the carbene carbon atom (H···C distance of 2.46 Å).

Scheme 5. Activation Free Energies (in kcal·mol^{-1}) of C–H Activation at Different Sites of 6a

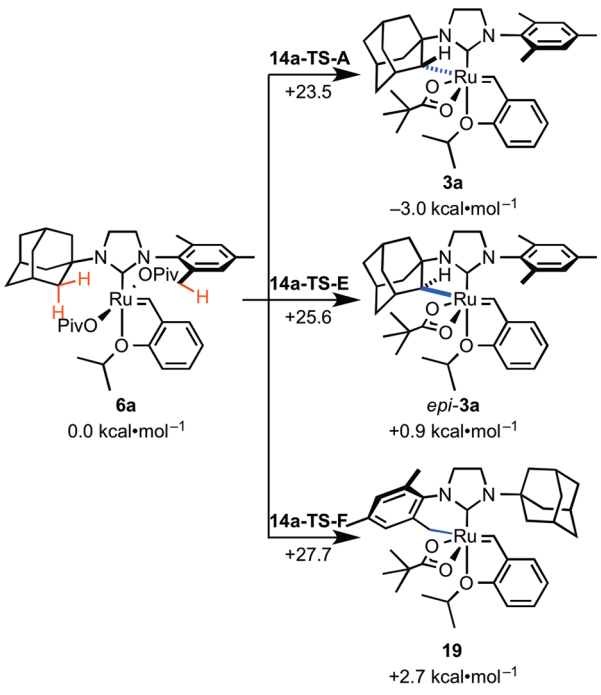

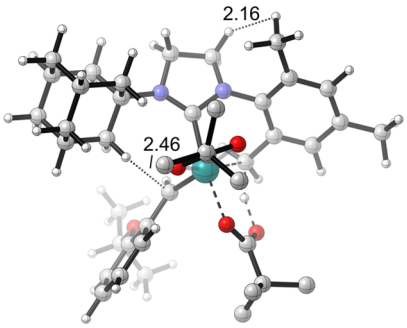

Figure 13. Transition-state geometry **14a-TS-F**.

In **14a-TS-A** and the resulting cyclometalated intermediate **3a**, the α-C–H bond on adamantyl is *anti* to the Ru-benzylidene double bond in a staggered conformation, while complexes **14a-TS-E** and *epi*-**3a** assume an eclipsed conformation with the α-C–H bond *syn* to the Ru-benzylidene bond (Figure 14). The staggered *anti* transition state **14a-TS-A**

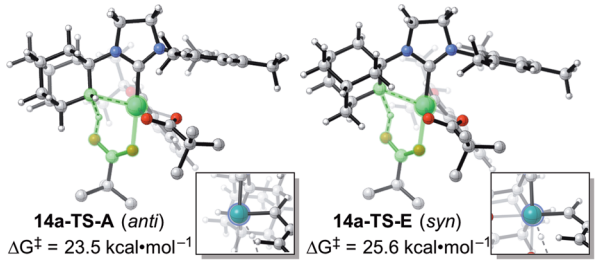

Figure 14. Comparison of the diastereomeric C–H activation transition states **14a-TS-A** (*anti*) and **14a-TS-E** (*syn*). Insets are Newman projections along the forming Ru–C bond. Energies are relative to **6a**.

is favored by 2.1 kcal·mol^{-1}. The *anti* intermediate **3a** is also more stable than the *syn* intermediate *epi*-**3a** to a greater extent (3.9 kcal·mol^{-1}).

Effects of *N*-Substituents on the Barriers for C–H Activation. Barriers for C–H activation with *N*-*t*-Bu-*N*′-Mes complex **6c** and *N*-Adm-*N*′-DIPP complex **6d** were computed (Figure 15). Replacing the adamantyl group with the smaller *tert*-butyl group significantly decreased the barrier to 15.2 kcal·mol^{-1}. There are fewer steric repulsions in the activation of the primary C–H bond in *t*-Bu than the secondary C–H bond on

dx.doi.org/10.1021/ja5021958 | J. Am. Chem. Soc. 2014, 136, 6733–6743

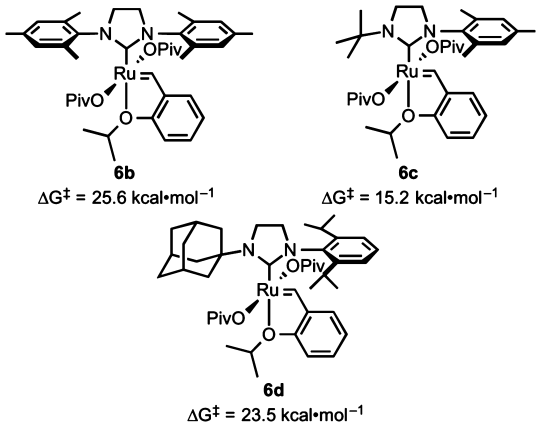

Figure 15. Computed activation barriers at 25 °C for cyclometalation of complexes **6b–d**.

adamantyl. This reactivity trend agrees with palladium-catalyzed C(sp^3)–H activations,[1b,2k,38] in which less-hindered primary C–H bonds are preferred. In contrast, iron oxo-catalyzed reactions are governed by a combination of steric and electronic effects.[39]

On the other hand, replacing the *N*-mesityl group with *N*-DIPP has negligible effects on the activation barrier. The *N*-mesityl and *N*-DIPP groups both remain perpendicular to the NHC ring in the dipivalate resting state and in the transition state. There are no significant steric repulsions with either the *N*-mesityl or *N*-DIPP group in the dipivalate complex or in the transition state.[40]

CONCLUSION

Studies in the development of a new family of *Z*-selective olefin metathesis catalysts revealed an interesting and relevant C–H activation reaction at ruthenium(II). This reaction involves a carboxylate-assisted concerted metalation–deprotonation via an organized six-membered metallacyclic transition state. The resulting ruthenium alkyl complexes are unusually stable, and these benzylidene complexes exhibit high levels of *Z*-selectivity in olefin metathesis reactions.

Isolation of the dicarboxylate complexes **6** allowed for the direct study of the C–H activation reaction. Kinetic studies revealed first-order reaction kinetics, and thermodynamic results agreed with computed transition states. Furthermore, $\Delta S^{\ddagger}$ values agree with a highly ordered intramolecular transition state. Computational studies revealed an interesting pseudo-apically oriented carboxylate geometry in the key cyclometalation step and confirmed that a second carboxylate ligand is necessary for transition-state stabilization. Electronic effects of the complex control the rate by modulating either the electron density at the ruthenium center or the overall basicity of the assisting carboxylate.

Experimental and computational results showed that steric effects control the site-selectivity of C–H activation, directing metalation toward typically less-reactive C–H bonds. The computational model was then able to corroborate indirect mechanistic evidence about the relative rates of cyclometalation at complexes that could not be studied directly.

New mechanistic information was developed regarding the inner-sphere activation of methylene C(sp^3)–H bonds. It is envisioned that the results of this study will enable the further development of CMD C(sp^3)–H activation at ruthenium centers both for the more efficient synthesis of selective ruthenium metathesis catalysts and for functionalization of C–H bonds in general.

ASSOCIATED CONTENT

Supporting Information

Experimental details, NMR spectra of new compounds, additional kinetics data, optimized Cartesian coordinates and energies, details of computational methods, and complete ref 26. This material is available free of charge via the Internet at http://pubs.acs.org.

AUTHOR INFORMATION

Corresponding Authors

doleary@pomona.edu
houk@chem.ucla.edu
rhg@caltech.edu

Notes

The authors declare no competing financial interest.

ACKNOWLEDGMENTS

This work was financially supported by the NIH (NIH R01-GM031332 and NRSA to J.S.C.: F32-GM103002), the NSF (CHE-1212767, CHE-1059084), and the NSF CCI Center for Stereoselective C–H Functionalization (CHE-1205646). NMR spectra were obtained by instruments supported by the NIH (RR027690). Materia, Inc. is acknowledged for the generous donation of complex **4b**. D.J.O. thanks Pomona College for supporting a portion of this research. Calculations were performed on the Hoffman2 cluster at UCLA and the Extreme Science and Engineering Discovery Environment (XSEDE), which is supported by the NSF. K. M. Engle, J. Hartung, and Z. K. Wickens are gratefully acknowledged for helpful discussions.

REFERENCES

(1) (a) Lapointe, D.; Fagnou, K. *Chem. Lett.* **2010**, *39*, 1118. (b) Lyons, T. W.; Sanford, M. S. *Chem. Rev.* **2010**, *110*, 1147. (c) Ackermann, L. *Chem. Rev.* **2011**, *111*, 1315. (d) Yamaguchi, J.; Yamaguchi, A. D.; Itami, K. *Angew. Chem., Int. Ed.* **2012**, *51*, 8960. (e) Neufeldt, S. R.; Sanford, M. S. *Acc. Chem. Res.* **2012**, *45*, 936. (f) Engle, K. M.; Mei, T.-S.; Wasa, M.; Yu, J.-Q. *Acc. Chem. Res.* **2012**, *45*, 788. (g) Yeung, C. S.; Dong, V. M. *Chem. Rev.* **2011**, *111*, 1215.

(2) (a) Canty, A. J.; Ariafard, A.; Sanford, M. S.; Yates, B. F. *Organometallics* **2013**, *32*, 544. (b) Lyons, T. W.; Hull, K. L.; Sanford, M. S. *J. Am. Chem. Soc.* **2011**, *133*, 4455. (c) Baxter, R. D.; Sale, D.; Engle, K. M.; Yu, J.-Q.; Blackmond, D. G. *J. Am. Chem. Soc.* **2012**, *134*, 4600. (d) Rousseaux, S.; Gorelsky, S. I.; Chung, B. K. W.; Fagnou, K. *J. Am. Chem. Soc.* **2010**, *132*, 10692. (e) Gorelsky, S. I.; Lapointe, D.; Fagnou, K. *J. Am. Chem. Soc.* **2008**, *130*, 10848. (f) Gorelsky, S. I.; Lapointe, D.; Fagnou, K. *J. Org. Chem.* **2012**, *77*, 658. (g) Sun, H.-Y.; Gorelsky, S. I.; Stuart, D. R.; Campeau, L.-C.; Fagnou, K. *J. Org. Chem.* **2010**, *75*, 8180. (h) Wakioka, M.; Nakamura, Y.; Hihara, Y.; Ozawa, F.; Sakaki, S. *Organometallics* **2013**, *32*, 4423. (i) García-Cuadrado, D.; Braga, A. A. C.; Maseras, F.; Echavarren, A. M. *J. Am. Chem. Soc.* **2006**, *128*, 1066. (j) Chen, X.; Engle, K. M.; Wang, D.-H.; Yu, J.-Q. *Angew. Chem., Int. Ed.* **2009**, *48*, 5094. (k) Daugulis, O.; Do, H.-Q.; Shabashov, D. *Acc. Chem. Res.* **2009**, *42*, 1074.

(3) (a) Davies, D. L.; Donald, S. M. A.; Al-Duaij, O.; Macgregor, S. A.; Pölleth, M. *J. Am. Chem. Soc.* **2006**, *128*, 4210. (b) Li, L.; Brennessel, W. W.; Jones, W. D. *Organometallics* **2009**, *28*, 3492. (c) Hartwig, J. F. *Acc. Chem. Res.* **2012**, *45*, 864. (d) Mkhalid, I. A. I.; Barnard, J. H.; Marder, T. B.; Murphy, J. M.; Hartwig, J. F. *Chem. Rev.* **2010**, *110*, 890.

(4) (a) Rhinehart, J. L.; Manbeck, K. A.; Buzak, S. K.; Lippa, G. M.; Brennessel, W. W.; Goldberg, K. I.; Jones, W. D. *Organometallics* **2012**,

31, 1943. (b) Davies, H. M. L.; Manning, J. R. *Nature* **2008**, *451*, 417. (c) Davies, H. M. L.; Morton, D. *Chem. Soc. Rev.* **2011**, *40*, 1857. (d) Colby, D. A.; Tsai, A. S.; Bergman, R. G.; Ellman, J. A. *Acc. Chem. Res.* **2012**, *45*, 814.

(5) (a) Davies, D. L.; Al-Duaij, O.; Fawcett, J.; Giardiello, M.; Hilton, S. T.; Russell, D. R. *Dalton Trans.* **2003**, 4132. (b) Arockiam, P. B.; Bruneau, C.; Dixneuf, P. H. *Chem. Rev.* **2012**, *112*, 5879. (c) Kozhushkov, S. I.; Ackermann, L. *Chem. Sci.* **2013**, *4*, 886. (d) Ackermann, L.; Vicente, R.; Potukuchi, H. K.; Pirovano, V. *Org. Lett.* **2010**, *12*, 5032. (e) Hashiguchi, B. G.; Young, K. J. H.; Yousufuddin, M.; Goddard, W. A., III; Periana, R. A. *J. Am. Chem. Soc.* **2010**, *132*, 12542. (f) Gruver, B. C.; Adams, J. J.; Warner, S. J.; Arulsamy, N.; Roddick, D. M. *Organometallics* **2011**, *30*, 5133.

(6) (a) Gephart, R. T., III; Warren, T. H. *Organometallics* **2012**, *31*, 7728. (b) Yamaguchi, J.; Muto, K.; Itami, K. *Eur. J. Org. Chem.* **2013**, 19.

(7) (a) Ryabov, A. D.; Sakodinskaya, I. K.; Yatsimirsky, A. K. *J. Chem. Soc., Dalton Trans.* **1985**, 2629. (b) Kurzeev, S. A.; Kazankov, G. M.; Ryabov, A. D. *Inorg. Chim. Acta* **2002**, *340*, 192. (c) Maleckis, A.; Kampf, J. W.; Sanford, M. S. *J. Am. Chem. Soc.* **2013**, *135*, 6618. (d) Sanhueza, I. A.; Wagner, A. M.; Sanford, M. S.; Schoenebeck, F. *Chem. Sci.* **2013**, *4*, 2767.

(8) (a) Davies, D. L.; Donald, S. M. A.; Macgregor, S. A. *J. Am. Chem. Soc.* **2005**, *127*, 13754. (b) García-Cuadrado, D.; de Mendoza, P.; Braga, A. A. C.; Maseras, F.; Echavarren, A. M. *J. Am. Chem. Soc.* **2007**, *129*, 6880. (c) Balcells, D.; Clot, E.; Eisenstein, O. *Chem. Rev.* **2010**, *110*, 749. (d) Ke, Z.; Cundari, T. R. *Organometallics* **2010**, *29*, 821. (e) Musaev, D. G.; Kaledin, A.; Shi, B.-F.; Yu, J.-Q. *J. Am. Chem. Soc.* **2012**, *134*, 1690. (f) Giri, R.; Lan, Y.; Liu, P.; Houk, K. N.; Yu, J.-Q. *J. Am. Chem. Soc.* **2012**, *134*, 14118. (g) Yang, Y.-F.; Cheng, G.-J.; Liu, P.; Leow, D.; Sun, T.-Y.; Chen, P.; Zhang, X.; Yu, J.-Q.; Wu, Y.-D.; Houk, K. N. *J. Am. Chem. Soc.* **2014**, *136*, 344. (h) Cheng, G.-J.; Yang, Y.-F.; Liu, P.; Chen, P.; Sun, T.-Y.; Li, G.; Zhang, X.; Houk, K. N.; Yu, J.-Q.; Wu, Y.-D. *J. Am. Chem. Soc.* **2014**, *136*, 894. (i) Sokolov, V. I.; Troitskaya, L. L.; Reutov, O. A. *J. Organomet. Chem.* **1979**, *182*, 537.

(9) (a) Prokopcová, H.; Bergman, S. D.; Aelvoet, K.; Smout, V.; Herrebout, W.; Van der Veken, B.; Meerpoel, L.; Maes, B. U. W. *Chem.—Eur. J.* **2010**, *16*, 13063. (b) Bergman, S. D.; Storr, T. E.; Prokopcová, H.; Aelvoet, K.; Diels, G.; Meerpoel, L.; Maes, B. U. W. *Chem.—Eur. J.* **2012**, *18*, 10393. (c) Kumar, N. Y. P.; Jeyachandran, R.; Ackermann, L. *J. Org. Chem.* **2013**, *78*, 4145. (d) Jun, C.-H.; Hwang, D.-C.; Na, S.-J. *Chem. Commun.* **1998**, 1405. (e) Dastbaravardeh, N.; Kirchner, K.; Schnürch, M.; Mihovilovic, M. D. *J. Org. Chem.* **2013**, *78*, 658. (f) Dastbaravardeh, N.; Schnürch, M.; Mihovilovic, M. D. *Org. Lett.* **2012**, *14*, 3792. (g) Chatani, N.; Asaumi, T.; Yorimitsu, S.; Ikeda, T.; Kakiuchi, F.; Murai, S. *J. Am. Chem. Soc.* **2001**, *123*, 10935. (h) Weissman, H.; Song, X.; Milstein, D. *J. Am. Chem. Soc.* **2001**, *123*, 337. (i) Oi, S.; Fukita, S.; Hirata, N.; Watanuki, N.; Miyano, S.; Inoue, Y. *Org. Lett.* **2001**, *3*, 2579. (j) Ozdemir, I.; Demir, S.; Çetinkaya, B.; Gourlaouen, C.; Maseras, F.; Bruneau, C.; Dixneuf, P. H. *J. Am. Chem. Soc.* **2008**, *130*, 1156. (k) Ackermann, L. *Org. Lett.* **2005**, *7*, 3123. (l) Padala, K.; Jeganmohan, M. *Org. Lett.* **2011**, *13*, 6144. (m) Burling, S.; Paine, B. M.; Nama, D.; Brown, V. S.; Mahon, M. F.; Prior, T. J.; Pregosin, P. S.; Whittlesey, M. K.; Williams, J. M. J. *J. Am. Chem. Soc.* **2007**, *129*, 1987. (n) Häller, L. J. L.; Page, M. J.; Macgregor, S. A.; Mahon, M. F.; Whittlesey, M. K. *J. Am. Chem. Soc.* **2009**, *131*, 4604.

(10) Diggle, R. A.; Kennedy, A. A.; Macgregor, S. A.; Whittlesey, M. K. *Organometallics* **2008**, *27*, 938.

(11) (a) Liang, J.-L.; Yuan, S.-X.; Huang, J.-S.; Yu, W.-Y.; Che, C.-M. *Angew. Chem., Int. Ed.* **2002**, *41*, 3465. (b) McNeill, E.; Du Bois, J. *J. Am. Chem. Soc.* **2010**, *132*, 10202. (c) Harvey, M. E.; Musaev, D. G.; Du Bois, J. *J. Am. Chem. Soc.* **2011**, *133*, 17207. (d) McNeill, E.; Du Bois, J. *Chem. Sci.* **2012**, *3*, 1810.

(12) (a) Ferrer Flegeau, E.; Bruneau, C.; Dixneuf, P. H.; Jutand, A. *J. Am. Chem. Soc.* **2011**, *133*, 10161. (b) Fabre, I.; von Wolff, N.; Le Duc, G.; Ferrer Flegeau, E.; Bruneau, C.; Dixneuf, P. H.; Jutand, A. *Chem.—Eur. J.* **2013**, *19*, 7595.

(13) (a) Keitz, B. K.; Endo, K.; Patel, P. R.; Herbert, M. B.; Grubbs, R. H. *J. Am. Chem. Soc.* **2012**, *134*, 693. (b) Endo, K.; Grubbs, R. H. *J. Am. Chem. Soc.* **2011**, *133*, 8525. (c) Rosebrugh, L. E.; Herbert, M. B.; Marx, V. M.; Keitz, B. K.; Grubbs, R. H. *J. Am. Chem. Soc.* **2013**, *135*, 1276. (d) Rosebrugh, L. E.; Marx, V. M.; Keitz, B. K.; Grubbs, R. H. *J. Am. Chem. Soc.* **2013**, *135*, 10032. (e) Endo, K.; Herbert, M. B.; Grubbs, R. H. *Organometallics* **2013**, *32*, 5128.

(14) Marx, V. M.; Herbert, M. B.; Keitz, B. K.; Grubbs, R. H. *J. Am. Chem. Soc.* **2013**, *135*, 94.

(15) (a) Herbert, M. B.; Marx, V. M.; Pederson, R. L.; Grubbs, R. H. *Angew. Chem., Int. Ed.* **2013**, *52*, 310. (b) Cannon, J. S.; Grubbs, R. H. *Angew. Chem., Int. Ed.* **2013**, *52*, 9001. (c) Quigley, B. L.; Grubbs, R. H. *Chem. Sci.* **2014**, *5*, 501.

(16) (a) Hartung, J.; Grubbs, R. H. *J. Am. Chem. Soc.* **2013**, *135*, 10183. (b) Hartung, J.; Grubbs, R. H. *Angew. Chem., Int. Ed.* **2014**, *53*, 3885.

(17) Miyazaki, H.; Herbert, M. B.; Liu, P.; Dong, X.; Xu, X.; Keitz, B. K.; Ung, T.; Mkrtumyan, G.; Houk, K. N.; Grubbs, R. H. *J. Am. Chem. Soc.* **2013**, *135*, 5848.

(18) (a) Meek, S. J.; O'Brien, R. V.; Llaveria, J.; Schrock, R. R.; Hoveyda, A. H. *Nature* **2011**, *471*, 461. (b) Flook, M. M.; Jiang, A. J.; Schrock, R. R.; Müller, P.; Hoveyda, A. H. *J. Am. Chem. Soc.* **2009**, *131*, 7962. (c) Marinescu, S. C.; Levine, D. S.; Zhao, Y.; Schrock, R. R.; Hoveyda, A. H. *J. Am. Chem. Soc.* **2011**, *133*, 11512. (d) Jiang, A. J.; Zhao, Y.; Schrock, R. R.; Hoveyda, A. H. *J. Am. Chem. Soc.* **2009**, *131*, 16630. (e) Yu, M.; Ibrahem, I.; Hasegawa, M.; Schrock, R. R.; Hoveyda, A. H. *J. Am. Chem. Soc.* **2012**, *134*, 2788.

(19) (a) Herbert, M. B.; Lan, Y.; Keitz, B. K.; Liu, P.; Endo, K.; Day, M. W.; Houk, K. N.; Grubbs, R. H. *J. Am. Chem. Soc.* **2012**, *134*, 7861. (b) Hong, S. H.; Chlenov, A.; Day, M. W.; Grubbs, R. H. *Angew. Chem., Int. Ed.* **2007**, *46*, 5148. (c) Mathew, J.; Koga, N.; Suresh, C. H. *Organometallics* **2008**, *27*, 4666. (d) Poater, A.; Cavallo, L. *J. Mol. Catal. A—Chem.* **2010**, *324*, 75. (e) Poater, A.; Bahri-Laleh, N.; Cavallo, L. *Chem. Commun.* **2011**, *47*, 6674. (f) Leitao, E. M.; Dubberley, S. R.; Piers, W. E.; Wu, Q.; McDonald, R. *Chem.—Eur. J.* **2008**, *14*, 11565.

(20) Krause, J. O.; Nuyken, O.; Wurst, K.; Buchmeiser, M. R. *Chem.—Eur. J.* **2004**, *10*, 777.

(21) (a) Ess, D. H.; Nielsen, R. J.; Goddard, W. A., III; Periana, R. A. *J. Am. Chem. Soc.* **2009**, *131*, 11686. (b) Ess, D. H.; Goddard, W. A., III; Periana, R. A. *Organometallics* **2010**, *29*, 6459.

(22) (a) Thiel, V.; Hendann, M.; Wannowius, K.-J.; Plenio, H. *J. Am. Chem. Soc.* **2012**, *134*, 1104. (b) Bujok, R.; Bieniek, M.; Masnyk, M.; Michrowska, A.; Sarosiek, A.; Stępowska, H.; Arlt, D.; Grela, K. *J. Org. Chem.* **2004**, *69*, 6894. (c) Van Veldhuizen, J. J.; Gillingham, D. G.; Garber, S. B.; Kataoka, O.; Hoveyda, A. H. *J. Am. Chem. Soc.* **2003**, *125*, 12502. (d) Zaja, M.; Connon, S. J.; Dunne, A. M.; Rivard, M.; Buschmann, N.; Jiricek, J.; Blechert, S. *Tetrahedron* **2003**, *59*, 6545.

(23) Sanford, M. S.; Love, J. A.; Grubbs, R. H. *J. Am. Chem. Soc.* **2001**, *123*, 6543.

(24) (a) Jones, W. D. *Acc. Chem. Res.* **2003**, *36*, 140. (b) Gómez-Gallego, M.; Sierra, M. A. *Chem. Rev.* **2011**, *111*, 4857. (c) Simmons, E. M.; Hartwig, J. F. *Angew. Chem., Int. Ed.* **2012**, *51*, 3066.

(25) Liu, P.; Xu, X.; Dong, X.; Keitz, B. K.; Herbert, M. B.; Grubbs, R. H.; Houk, K. N. *J. Am. Chem. Soc.* **2012**, *134*, 1464.

(26) Frisch, M. J.; et al. *Gaussian 09*, Revision B.01; Gaussian, Inc.: Wallingford, CT, 2009.

(27) Ragone, F.; Poater, A.; Cavallo, L. *J. Am. Chem. Soc.* **2010**, *132*, 4249.

(28) Ackermann, L.; Vicente, R.; Althammer, A. *Org. Lett.* **2008**, *10*, 2299.

(29) (a) Bischof, S. M.; Ess, D. H.; Meier, S. K.; Oxgaard, J.; Nielsen, R. J.; Bhalla, G.; Goddard, W. A., III; Periana, R. A. *Organometallics* **2010**, *29*, 742. (b) Ess, D. H.; Gunnoe, T. B.; Cundari, T. R.; Goddard, W. A., III; Periana, R. A. *Organometallics* **2010**, *29*, 6801. (c) Ess, D. H.; Bischof, S. M.; Oxgaard, J.; Periana, R. A.; Goddard, W. A., III *Organometallics* **2008**, *27*, 6440.

(30) The outer-sphere deprotonation transition state may be stabilized by coordination of solvent molecules with the unbound pivalate. Because of the implicit solvation model used in this study, the

energy difference between **14a-TS-D** and **14a-TS-A** might be overestimated.
(31) Saunders, M.; Laidig, K. E.; Wolfsberg, M. *J. Am. Chem. Soc.* **1989**, *111*, 8989.
(32) (a) Bigeleisen, J.; Mayer, M. G. *J. Chem. Phys.* **1947**, *15*, 261. (b) Bigeleisen, J.; Wolfsberg, M. *Adv. Chem. Phys.* **1958**, *1*, 15.
(33) Halls, M. D.; Tripp, C. P.; Schlegel, H. B. *Phys. Chem. Chem. Phys.* **2001**, *3*, 2131.
(34) Carboxylates have minimal effects on the de-chelation of the benzylidene chelate. The energy difference between **6a** and **13a** is 6.7, 6.7, and 6.4 kcal·mol^{-1} respectively for pivalate, acetate, and benzoate.
(35) For details, see the Supporting Information.
(36) The energy differences between the Hoveyda chelate (**10a−d**) and the C−H coordinated complex (analogue of **13a**) are similar (5.3, 5.5, 6.7, and 4.7 kcal·mol^{-1} respectively for X = OMe, Me, H, and Cl).
(37) For computational investigations on regioselectivity in palladium carboxylate-catalyzed C−H activations: (a) Guihaumé, J.; Clot, E.; Eisenstein, O.; Perutz, R. N. *Dalton Trans.* **2010**, *39*, 10510. (b) Petit, A.; Flygare, J.; Miller, A. T.; Winkel, G.; Ess, D. H. *Org. Lett.* **2012**, *14*, 3680.
(38) (a) Baudoin, O.; Herrbach, A.; Guéritte, F. *Angew. Chem., Int. Ed.* **2003**, *42*, 5736. (b) Giri, R.; Maugel, N.; Li, J.-J.; Wang, D.-H.; Breazzano, S. P.; Saunders, L. B.; Yu, J.-Q. *J. Am. Chem. Soc.* **2007**, *129*, 3510.
(39) (a) Chen, M. S.; White, M. C. *Science* **2010**, *327*, 566. (b) Hitomi, Y.; Arakawa, K.; Funabiki, T.; Kodera, M. *Angew. Chem., Int. Ed.* **2012**, *51*, 3448. (c) Bigi, M. A.; Liu, P.; Zou, L.; Houk, K. N.; White, M. C. *Synlett* **2012**, *23*, 2768. (d) Prat, I.; Gómez, L.; Canta, M.; Ribas, X.; Costas, M. *Chem.—Eur. J.* **2013**, *19*, 1908.
(40) See the Supporting Information for 3D structures of complexes **14b-TS**, **14c-TS**, and **14d-TS**.